Processing and Application of Ceramics 16 [4] (2022) 384–390
https://doi.org/10.2298/PAC2204384Y

The influence of carbon source and content on structure and mechanical properties of SiC processed via spark plasma sintering method

Zeynep Aygüzer Yaşar[1], Vincent A. DeLucca[2], Richard A. Haber[1,*]

[1]*Department of Material Science and Engineering, Rutgers, The State University of New Jersey, Piscataway, NJ 08854,USA*
[2]*Greenleaf Corporation, Saegertown, PA, 16433, USA*

Received 8 July 2022; Received in revised form 28 September 2022; Accepted 28 October 2022

Abstract

The effects of carbon sources and carbon content on the density, microstructure, hardness and elastic properties of dense SiC ceramics were investigated. The precursor powders were prepared by adding 1.5–4.5 wt.% C (carbon lamp black or phenolic resin) and 0.5 wt.% B_4C to SiC and sintered at 1900 °C for 15 min under 50 MPa pressure in argon with an intermediate dwell at 1400 °C for 30 min. The results showed that carbon lamp black provided better mixing than phenolic resin since carbon cluster was found in the samples made with phenolic resin. Increasing carbon content causes the decrease of 4H polytype amount in the samples. The presence of higher than 1.5 wt.% carbon inhibits grain growth and the presence of the 4H polytype. SiC samples can be produced with relative density of more than 99 %TD with 1.5 wt.% carbon lamp black addition which shows small average grain size, high elastic modulus and hardness of 2.28 μm, 453 GPa and 21.2 GPa, respectively.

Keywords: *silicon carbide, sintering, spark plasma sintering, solid state, microstructure*

I. Introduction

Dense SiC ceramics can be used in many applications since it has a low density (3.21 g/cm^3), a low coefficient of thermal expansion, high thermal conductivity, high melting point, high hardness, high wear resistance and high elastic modulus [1–19].

In addition to having these superior properties, due to its strong covalent structure densifying the SiC is very difficult [9,20]. In order to obtain highly dense SiC, sintering aids can be added, or pressure sintering methods can be used [21–26]. However, studies have shown that high density could not be obtained by pressure assisted sintering without sintering aids [27].

The choice of sintering aid materials has a great impact on the properties of sintered SiC, and these materials determine whether the material will densify by liquid phase sintering or solid state sintering. While the use of Al_2O_3, Y_2O_3 and other rare earth oxides causes the formation of a liquid phase, using aluminium, boron and carbon enables SiC to sinter in the solid state [23,28–31]. Boron and carbon in particular are remarkable among these contributions. The addition of boron into SiC increases the self- diffusion coefficients of Si and C, resulting in enhanced densification [32]. It has been observed that the addition of C is very important to have dense SiC ceramics. C both removes the oxide layer on the surface of SiC by reacting with SiO_2 and prevents the formation of large grains and grain growth [25,28,30,31,33]. However, addition of B_4C to SiC without C causes glassy phase formation [25]. Therefore, these two additives should be added together to SiC since studies have shown that SiC produced by solid state sintering has a wide range of uses since SiC sintered by the solid-state method can be produced without losing its superior properties [7,13,17,25,34,35]. Even if SiC is produced using these two additives, the additive ratios must be adjusted well, otherwise SiC with large grain size will be obtained and the elastic modulus and hardness of these SiC will be low [35].

* Corresponding author: tel: +1 848 445 4931
e-mail: *rich.haber@rutgers.edu*

The aim of this research is to examine the effects of carbon sources and carbon content on the elastic and mechanical properties of SiC and obtain high dense SiC with superior features. To achieve this goal, two different carbon sources (carbon lamp black and phenolic resin) 1.5–4.5 wt.% and 0.5 wt.% B_4C were used as sintering aids to sinter SiC. The powder mixtures were solid state sintered via SPS at 1900 °C for 15 min under 50 MPa pressure in argon with an intermediate dwell at 1400 °C for 30 min. Then the density, microstructure, hardness and elastic properties of the dense SiC samples were analysed by Archimedes, FESEM, Knoop hardness indentation, and ultrasound analysis methods, respectively.

II. Experimental

Submicron α-SiC (UF-25, H. C. Starck GmbH&Co, Germany), 0.5 wt.% B_4C (HD-20, H. C. Starck GmbH&Co, Germany) and 1.5–4.5 wt.% C from two different sources, carbon lamp black (Fisher Scientific, USA) and phenolic resin (VARCUM 29353, Durez Corp.), were used as starting materials. The samples made using the lamp black carbon source are designated as HC-LBC and those made with the phenolic resin carbon source are designated as HC-PRC. The precursor powders were mixed by ball milling for 24 h in ethanol with SiC ball media. In order to remove the media from the liquid mixture, 1.4 mm mesh sieve was used. Then the liquid mixture was allowed to dry on a hot plate at 275 °C.

Thermogravimetric analysis (TGA) was performed on the phenolic resin in inert gas, in order to determine the carbon content. The TGA analysis (Fig. 1) showed that the char yield was approximately 43% and indicated that 2.58 times more phenolic resin had to be added to the HC-PRC series in order to end up with the same amount of carbon as in the HC-LBC series.

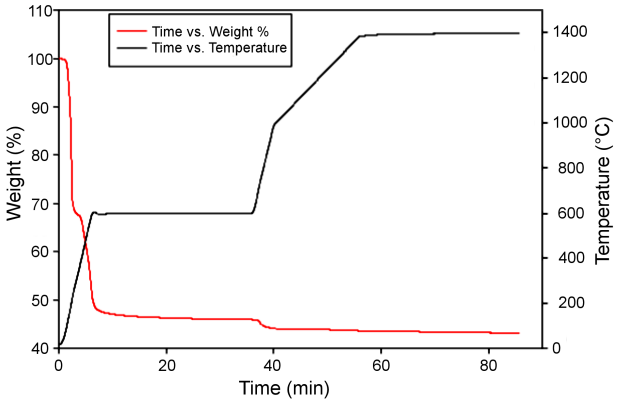

Figure 1. VARCUM phenolic resin TGA data

In order to make the phenolic resin ready for use, liquid phenolic resin was mixed with deionized water and sonicated. Then SiC and B_4C dry powders were mixed with ethanol and ammonium hydroxide (0.22 g) and SiC milling media was added to the mixture and mixed by ball milling for 24 h. The SiC media was separated from the liquid mixture using a sieve. In order to remove the surplus water, the liquid mixture was filter pressed at 2.4 bar and placed in an oven at 100 °C to dry.

Each sample was produced from 6.5 g of the prepared powder and the powders were placed in a 20 mm inner diameter graphite die and sintered via a Thermal Technology SPS 10-4 spark plasma sintering unit (Thermal Technology, LLC, Santa Rosa, CA, USA). The die was covered with graphite foil to prevent possible reaction between the powder and die. All samples were sintered at 1900 °C, but due to the different carbon usage, two different heating schedules were followed when densifying samples.

To densify the samples made with the LBC carbon source, the heating rate during the whole process was 200 °C/min and the pressure was 50 MPa. First, SPS was heated to 1400 °C and held for 30 min under vacuum, then argon was filled back into the SPS chamber and heated to 1900 °C and held for 15 min.

To densify the samples made with the PRC carbon source, the heating rate during the whole process was 200 °C/min. First of all, the SPS was heated to 800 °C under vacuum and held for 1 h under 20 MPa pressure to convert the phenolic resin to carbon. SPS was heated to 1400 °C and held for 30 min under vacuum and applied pressure of 50 MPa, then argon was filled back into the SPS chamber and heated to 1900 °C under 50 MPa and held for 15 min.

After densification, the dense samples needed sandblasting to remove excess graphite foil. However, after sandblasting, the surface of samples become very rough, so the surfaces of the samples were ground flat using a surface grinder with a 600 grit diamond wheel. It was cut into small pieces using a LECO VC-50 diamond saw (LECO Corporation, St. Joseph, MI, USA). The small cut pieces are mounted in epoxy using a Buehler SimpliMet 1000 mounting press (Buehler, Lake Bluff, IL, USA), and using Buehler- Ecomet 250-Grinder-Polisher with AutoMet 250 automatic head, all samples were polished (0.25 µm finish). In addition to polishing, the samples were ion milled using the flat-milling mode with 3 kV acceleration voltage, 80° tilt angle, no offset, and 25 rpm rotation speed for 10 min using a Hitachi IM4000 (Hitachi High-Technologies Corporation, Tokyo, Japan) to get better EBSD maps. To better visualize the grain boundaries of the samples in FESEM, they were highlighted by etching using a modified Murakami method (20 g KOH and 20 g $K_3Fe(CN)_6$ in 60 ml deionized water).

Densities of the samples were measured using the Archimedes method. All samples were cleaned using acetone and dried for 1 h in a drying oven. Each sample was weighed five times dry with Adam PGW analytical balance with 0.001 g accuracy. Then the samples were suspended five times in water. Elastic properties of the dense samples were measured by ultrasound analysis according to ASTM standard E494-10 [36]. The hardness of the dense samples were measured by making 10

indents each at loads of 100, 200, 500, 1000 and 2000 g using a Knoop diamond indenter with a LECO microhardness tester. A Keyence VHX5000 digital microscope (Keyence Corporation, Osaka, Japan) was used to measure the sizes of the indents. The microstructure of the samples was examined using Zeiss Sigma field emission scanning electron microscope (FESEM). An Oxford Instruments Nordlys Nano EBSD detector (Oxford Instruments, Abingdon, UK) on the Zeiss Sigma FESEM was used to collect the electron backscatter diffraction (EBSD) map of each sample. The EBSD technique was used to determine grain orientation and phase and polytype composition. The average grain size of each sample was measured using Lince 2.42 software using a minimum of 100 intersections using the linear intersept method.

III. Results and discussion

The microstructure of the SiC ceramics without sintering aids can be seen in Fig. 2. The sample had large pores and it is obvious that SiC could not reach high density without B_4C and C addition.

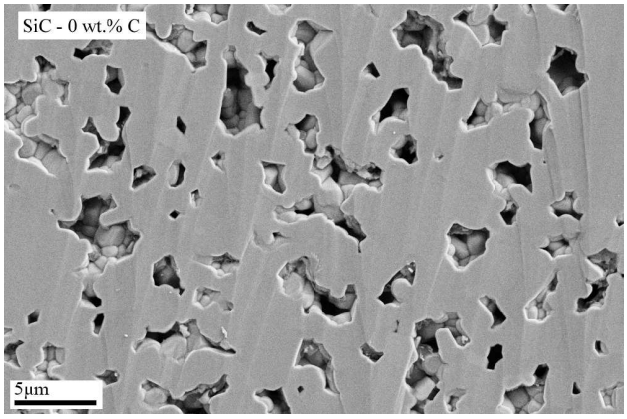

Figure 2. Microstructure of sintered SiC without additives

Figure 3 shows microstructures of the HC-LBC samples. The microstructure images showed that the sample made with the lowest carbon content (1.5 wt.%) was almost completely dense. On the other hand, the samples made with higher carbon content had some porosity. The microstructure images of the sample with 1.5% of carbon did not show residual carbon, however, the microstructure images of the 3.0% C and 4.5% C samples showed a significant amount of remaining carbon. The average grain size of the samples was similar, but the morphology of grains was changed with the addition of different carbon content. The 1.5% sample showed mainly equiaxed grains with some elongated grains. The samples made with higher carbon contents (3.0% and 4.5%) showed equiaxed grains. The average grain sizes of the samples are presented in Table 1. Even though the 1.5% carbon sample contained elongated grains, it had a similar average grain size to the samples with 3.0% and 4.5%, i.e. the average grain sizes were 2.28 ± 1.91, 2.41 ± 0.33 and 2.55 ± 0.72 µm, respectively. When the microstructure image of the 1.5% sample was compared with the images of the other samples, differences were observed in the grain shape. Thus, excess carbon in other samples may play a role in preventing grain elongation in these samples.

Microstructures of the HC-PRC samples are also shown in Fig. 3. Visible porosity was present in all samples of the HC-PRC series. However, the 1.5% sample had many smaller pores compared to other samples, while the 3% and 4.5% samples had larger sized pores. The sample with 1.5% C showed very small grain size. With increase of carbon content, the grain size increased and showed some elongation, thus the grain size and shape of the 3.5% and 4.5% samples were similar. The average grain sizes of the samples containing 1.5%, 3% and 4.5% C were 1.59 ± 0.30, 3.17 ± 0.67 and 3.32 ± 0.35 µm, respectively (Table 2).

The HC-PRC samples with 3.0% and 4.5% C showed

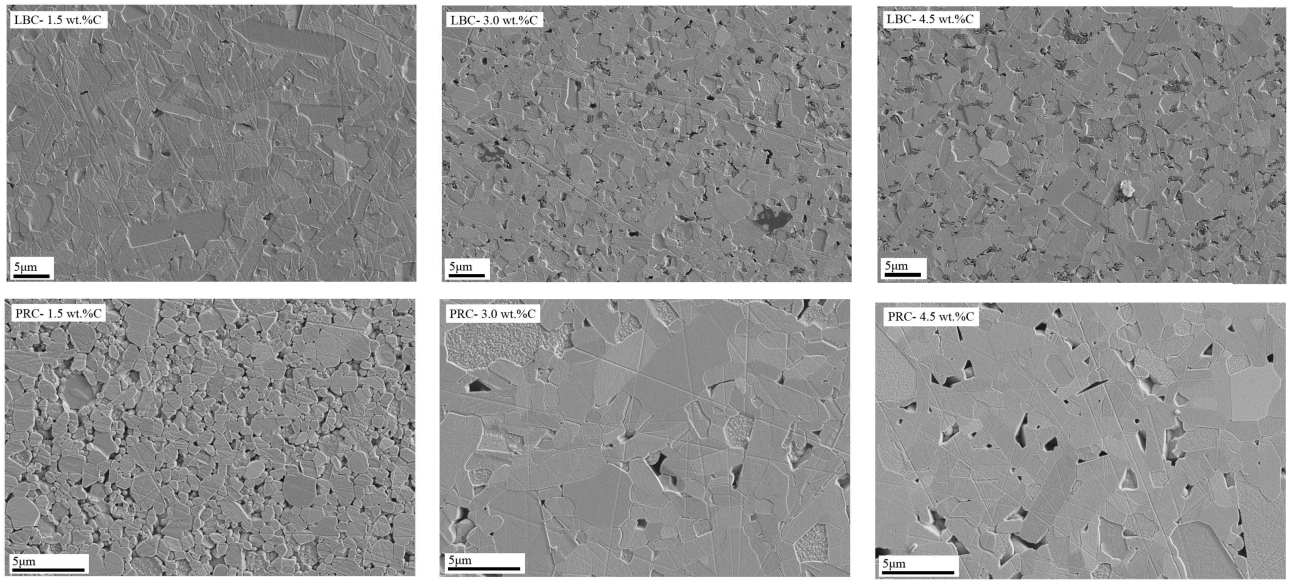

Figure 3. Microstructure of HC-LBC and HC-PRC series

Table 1. Microstructural features and elastic properties of HC-LBC series

Sample	Density [g/cm^3]	Average grain size [μm]	Phase fraction 4H [%]	Phase fraction 6H [%]	4H/6H ratio	*E* [GPa]
HC-0C	2.95	-	-	-	-	-
HC-LBC-1.5C	3.20	2.28 ± 1.91	23	53	0.43	453
HC-LBC-3.0C	3.16	2.41 ± 0.33	14	60	0.23	401
HC-LBC-4.5C	3.13	2.55 ± 0.72	13	54	0.24	363

Table 2. Microstructural features and elastic properties of HC-PRC series

Sample	Density [g/cm^3]	Average grain size [μm]	Phase fraction 4H [%]	Phase fraction 6H [%]	4H/6H ratio	*E* [GPa]
HC-0C	2.95	-	-	-	-	-
HC-PRC-1.5C	3.17	1.59 ± 0.30	10	26	0.38	424
HC-PRC-3.0C	3.15	3.17 ± 0.67	16	62	0.26	426
HC-PRC-4.5C	3.14	3.32 ± 0.35	13	57	0.23	422

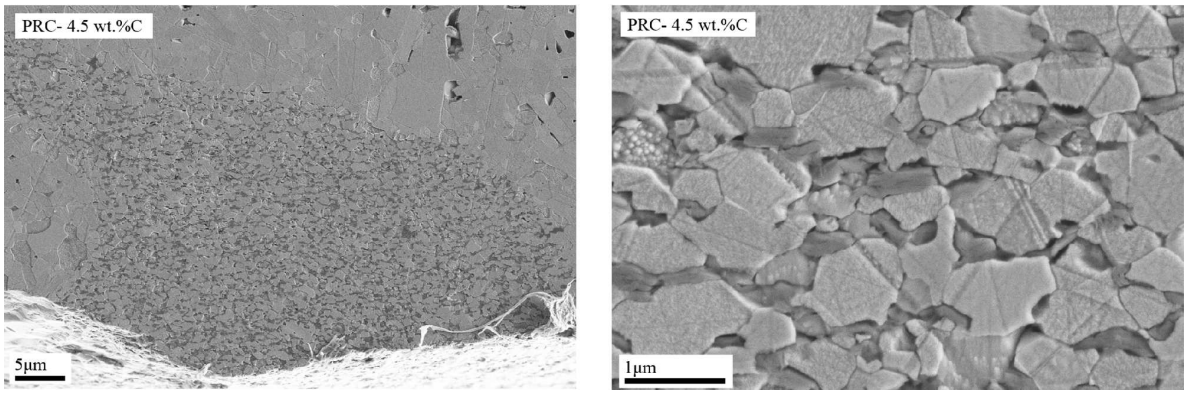

Figure 4. Microstructure of cluster formed in HC-PRC samples

a similar microstructure. However, the 4.5% sample had some large clusters of carbon inclusions that the 3.0% sample did not have. This cluster can be seen in Fig. 4. Similar cluster appearance was seen in the study of comparing the mixing methods of SiC [12]. This cluster is formed due to the improper mixing of carbon. Due to the presence of these clusters, it can be seen that the phenolic resin caused worse mixing than the lamp black carbon source.

EBSD maps of the HC-LBC samples can be seen in Fig. 5. In each map, 6H SiC polytype is shown in red colour and 4H polytype is shown in green colour based on the program. Black colour indicates areas where no SiC phase is detected due to the presence of secondary phases, pores, roughness, grain boundaries or other factors. It can be seen from the EBSD maps that the samples mostly have the 6H polytype and a small amount of the 4H polytype. When 6H-4H polytype contents of the samples are compared, long grains of the 4H polytype are more numerous in the 1.5% C sample than in the others. The phase fractions of each polytype found in these mapped areas are shown in Table 1. In theory, the total area of 6H and 4H can be expected to be 100%. However, for the reasons mentioned before (pores, grain boundaries, etc.), the sum of 6H and 4H does not add up to 100%. For the 3.0% and 4.5% samples, the ratio of 4H/6H SiC was quite low and the values were 0.23 and 0.24, respectively, whereas the 1.5% sample showed a higher 4H/6H ratio of 0.43. Thus, as the amount of carbon increased, less of the 4H polytype was detected in the sample. It can be said that the presence of residual carbon inhibits grain growth and the presence of the 4H polytype.

EBSD maps of the HC-PRC samples can be seen in Fig. 6. The EBSD maps showed mainly 6H polytype and small amount of 4H polytype. The phase fractions of each polytype samples are in Table 2. As mentioned above, the total areas of 6H and 4H do not add up to 100% due to the pores, grain boundaries and other factors. For the 3.0% and 4.5% samples, the ratio of 4H/6H SiC was quite low and the values were 0.26 and 0.23, respectively. The sample with 1.5% C showed slightly higher 4H/6H ratio of 0.38. However, due to the presence of porosities and residual carbon in the structure, there is a very large area where no SiC polytype was detected. The amount of added carbon appears to have some effect on polytype conversion. As the added carbon increases, the 4H/6H ratio decreases.

The densities and elastic moduli of the HC-LBC samples are shown in Table 1. Relative densities of the samples first increased with the addition of 1.5% C, then decreased with increasing the amount of carbon. The density of SiC without additives could only reach 92%. The highest density was obtained for the sample with 1.5% C and it was 99.69 %TD, whereas relative density values for the 3.0% and 4.5% samples were 98.44 and

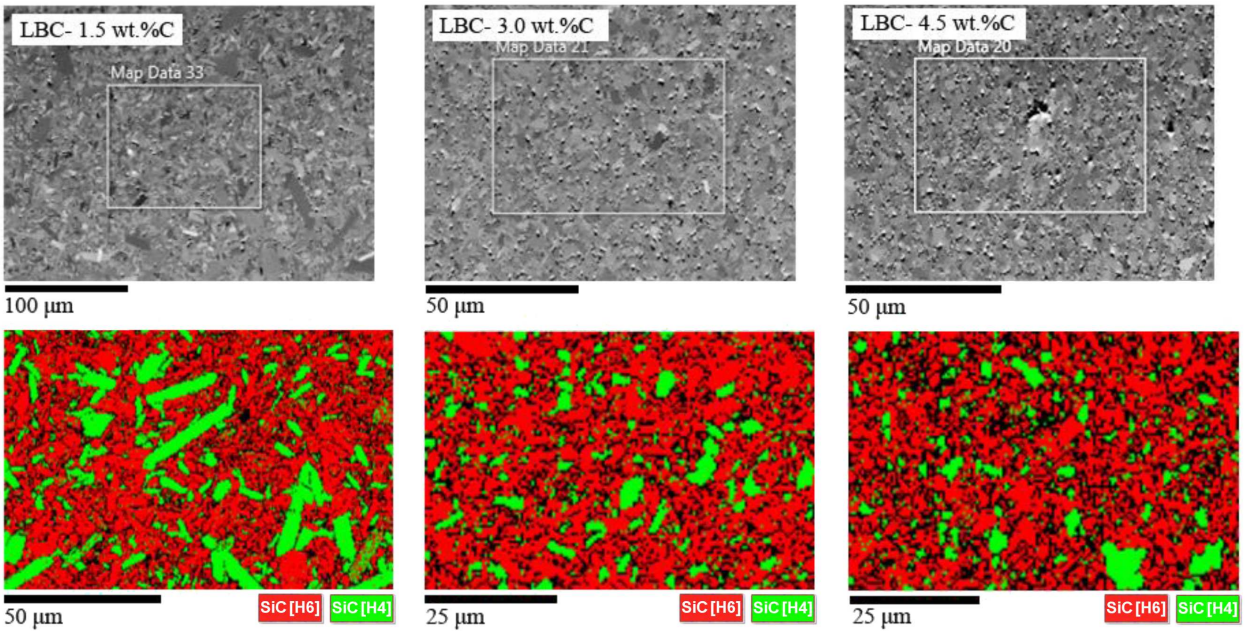

Figure 5. EBSD maps of HC-LBC series

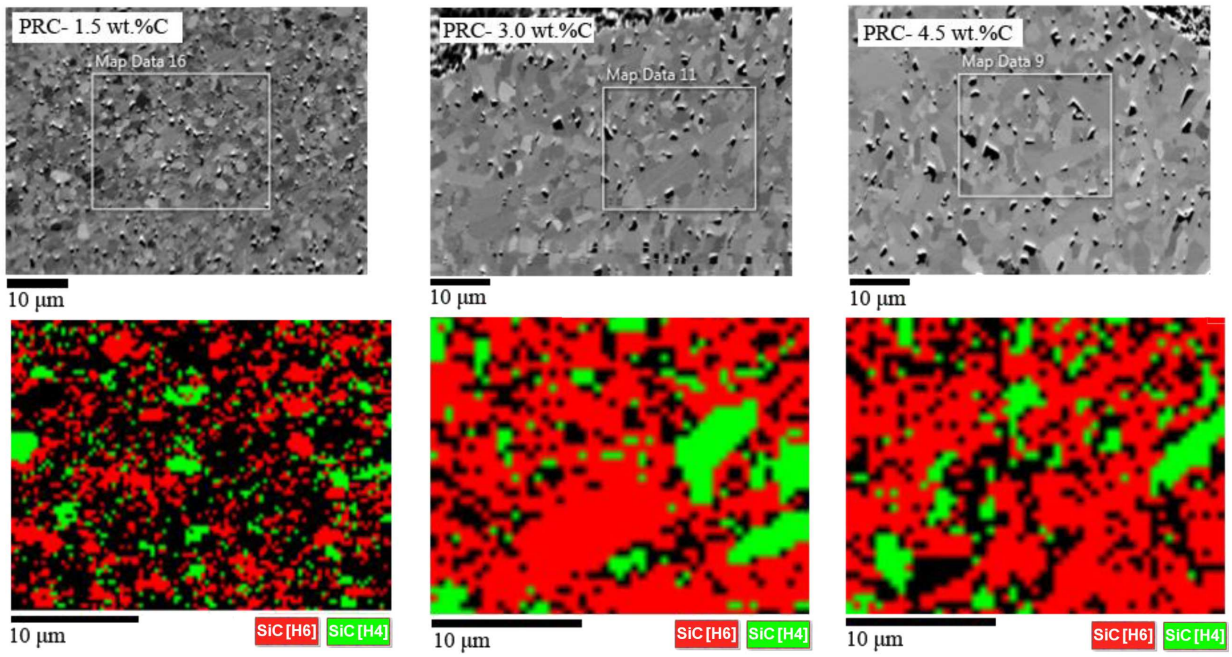

Figure 6. EBSD maps of HC-PRC series

97.50 %TD, respectively. In the literature, SiC sintered without additives with SPS only could reach the density of 91 %TD [37]. In the Li *et al.* [38] research, the importance of adding carbon to SiC was also confirmed. In the study, SiC sintered with the addition of B_4C reached density of only 98.6 %TD.

The elastic modulus of the samples also decreased with increasing carbon addition. Since the SiC sintered without sintering aids had many pores, its elastic and mechanical properties could not be measured. The highest value was 453 GPa for the 1.5% sample. The elastic modulus drastically decreased for the 3.0% and 4.5% samples to 401 and 363 GPa, respectively. It was clearly observed that elastic modulus and density values were inversely related to carbon content. It can be inferred that the residual carbon in the microstructure of these samples reduces the elastic modulus.

The densities and elastic moduli of the HC-PRC samples are shown in Table 2. Relative densities of the samples decreased with increasing the addition of carbon, as expected. The highest density was obtained for the sample with 1.5% C, and it was >98.75 %TD, while relative density values for the 3.0% and 4.5% samples were 98.13 and 97.81 %TD, respectively. However, the negative trend between the elastic modulus and carbon content of the HC-LBC samples was not observed in the

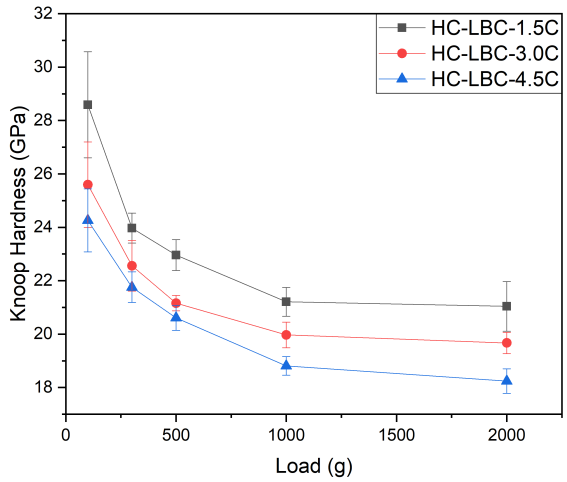

Figure 7. Knoop hardness values of HC-LBC series

HC-PRC samples. The elastic properties of these three samples are very similar. This suggests that the samples were similar and that the carbon clusters may not have been interrogated by the ultrasound beam where measurements were taken.

The hardness values of the HC-LBC series for each load (100, 300, 500, 1000 and 2000 g) are shown in Fig. 7. Since the 1.5% sample had the highest density, it showed for all loads higher hardness values than the other samples. Similar to the trend in elastic modulus, the hardness values decreased with the increasing addition of carbon for all applied loads. This is probably due to the residual carbon in the samples with higher carbon content as carbon has a lower hardness value than SiC, resulting in a decrease in hardness.

The hardness values of the HC-PRC series for each load (100, 300, 500, 1000 and 2000 g) are shown in Fig. 8. All samples' hardness values decreased with the increasing applied load. Similar to the trend seen in elastic modulus, the hardness values of the HC-PRC series were similar.

Even though the hardness values in both series were similar, some differences cannot be only explained with the differences in porosity [39], but also to different amount of residual carbon or grain size.

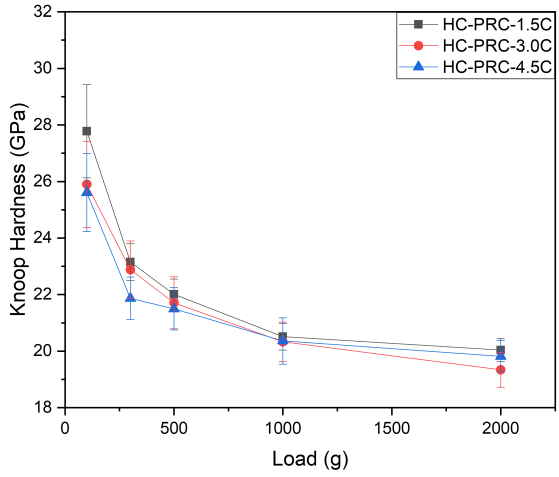

Figure 8. Knoop hardness values of HC-PRC series

IV. Conclusions

Dense SiC ceramics were prepared by mixing α-SiC with 0.5 wt.% B_4C and 1.5–4.5 wt.% C from two different sources (carbon lamp black and phenolic resin). The dry powder mixtures were sintered at 1900 °C for 15 min under 50 MPa pressure in argon with an intermediate dwell at 1400 °C for 30 min.

The results showed that carbon lamp black (samples of HC-LBC series) provided better mixing than phenolic resin (samples of HC-PRC series). For the HC-LBC series, the addition of carbon greater than 1.5 wt.% caused residual carbon on the microstructure and prevented the development of high elastic and mechanical properties. For the HC-PRC series, since the phenolic resin did not provide a uniform mixing as much as carbon lamp black, the addition of carbon more than 1.5 wt.% caused larger clusters of carbon and these were detrimental to high elastic and mechanical properties. It was also observed that the amount of carbon added had an effect on the 6H-4H ratio. As the amount of carbon added increased, less 4H polytype was detected in the samples. It can be said that the presence of residual carbon inhibits grain growth and the presence of the 4H polytype.

It was also seen that >99 %TD dense SiC ceramics can be fabricated with 1.5 wt.% carbon lamp black addition. The smallest average grain size, the highest elastic modulus and hardness value were also obtained in this sample (from the HC-LBC series), i.e. 2.28 µm, 453 GPa and 21.2 GPa, respectively.

Acknowledgements: The research was sponsored by the National Science Foundation I/UCRC Award No. 1540027. The views and conclusions contained in this document are those of the authors and should not be interpreted as representing the official policies, either expressed or implied, of the National Science Foundation or the U.S. Government. The U.S. Government is authorized to reproduce and distribute reprints for Government purposes notwithstanding any copyright notation herein. Additional funding was provided by the Materials for Extreme Dynamic Environments program sponsored by the US Army Research Laboratory Cooperative Agreement (W911NF-12-2-0022).

References

1. C. Schmalzried, K.A. Schwetz, "Silicon carbide-and boron carbide-based hard materials", pp. 131–227, Ch. 4 in *Ceramics Science and Technology, Volume 2: Materials and Properties*. Eds. R. Riedel, I.-W. Chen, Wiley-VCH Verlag GmbH & Co. KGaA, 2010.
2. A.K. Agarwal, S.E. Saddow, *Advances in silicon carbide processing and applications*, Artech House, USA, 2004.
3. V. Paris, N. Frage, M. Dariel, E. Zaretsky, "The spall strength of silicon carbide and boron carbide ceramics pro-

cessed by spark plasma sintering", *Int. J. Impact Eng.*, **37** (2010) 1092–1099.
4. J. Zhang, D. Jiang, Q. Lin, Z. Chen, Z. Huang, "Properties of silicon carbide ceramics from gelcasting and pressureless sintering", *Mater. Des.*, **65** (2015) 12–16.
5. H. Liang, X. Yao, Z. Huang, Y. Zeng, B. Su, "Effect of sintering techniques on the microstructure of liquid-phase-sintered SiC ceramics", *J. Eur. Ceram. Soc.*, **36** (2016) 1863–1871.
6. B. Lanfant, Y. Leconte, G. Bonnefont, V. Garnier, Y. Jorand, S. Le Gallet, M. Pinault, N. Herlin-Boime, F. Bernard, G. Fantozzi, "Effects of carbon and oxygen on the spark plasma sintering additive-free densification and on the mechanical properties of nanostructured SiC ceramics", *J. Eur. Ceram. Soc.*, **35** (2015) 3369–3379.
7. P. Barick, D. Chakravarty, B.P. Saha, R. Mitra, S.V. Joshi, "Effect of pressure and temperature on densification, microstructure and mechanical properties of spark plasma sintered silicon carbide processed with β-silicon carbide nanopowder and sintering additives", *Ceram. Int.*, **42** (2016) 3836–3848.
8. V. Izhevskyi, L. Genova, J. Bressiani, A. Bressiani, "Silicon carbide, structure, properties and processing", *Cerâmica*, **46** (2000) 4–13.
9. E. Halac, E. Burgos, H. Bonadeo, "Static and dynamical properties of SiC polytypes", *Phys. Rev. B*, **65** (2002) 125202.
10. K.K. Saxena, S. Agarwal, S.K. Khare, "Surface characterization, material removal mechanism and material migration study of micro EDM process on conductive SiC", *Procedia CIRP*, **42** (2016) 179–184.
11. K. Biswas, "Liquid phase sintering of SiC ceramics with rare earth sesquioxides", *Ph.D. thesis*. University of Stuttgart, Germany, 2002.
12. Z.A. Yaşar, R.A. Haber, "Effect of carbon addition and mixture method on the microstructure and mechanical properties of silicon carbide", *Materials*, **13** (2020) 3768.
13. K. Raju, D.-H. Yoon, "Sintering additives for SiC based on the reactivity: a review", *Ceram. Int.*, **42** (2016) 17947–17962.
14. I. Ogawa, K. Nishikubo, T. Imamura, "Growth of graphite particles in carbon/SiC/B_4C composites", *Carbon*, **37** (1999) 1000–1002.
15. S. Hayun, V. Paris, R. Mitrani, S. Kalabukhov, M. Dariel, E. Zaretsky, N. Frage, "Microstructure and mechanical properties of silicon carbide processed by Spark Plasma Sintering (SPS)", *Ceram. Int.*, **38** (2012) 6335–6340.
16. K. Yamada, M. Mohri, "Properties and applications of silicon carbide ceramics", pp. 13–44, Ch. 2 in *Silicon carbide ceramics - 1*. Eds. S. Sömiya, Y. Inomata, Springer, Dordrecht, The Netherlands, 1991.
17. Moskovskikh, Y. Song, S. Rouvimov, A. Rogachev, A. Mukasyan, "Silicon carbide ceramics: Mechanical activation, combustion and spark plasma sintering", *Ceram. Int.*, **42** (2016) 12686–12693.
18. P. Šajgalík, J. Sedláček, Z. Lenčéš, J. Dusza, H.-T. Lin, "Additive-free hot-pressed silicon carbide ceramics - A material with exceptional mechanical properties", *J. Eur. Ceram. Soc.*, **36** (2016) 1333–1341.
19. G. Magnani, A. Brentari, E. Burresi, G. Raiteri, "Pressureless sintered silicon carbide with enhanced mechanical properties obtained by the two-step sintering method", *Ceram. Int.*, **40** (2014) 1759–1763.
20. R. Hamminger, "Carbon inclusions in sintered silicon carbide", *J. Am. Ceram. Soc.*, **72** (1989) 1741–1744.
21. K. Schwetz, "Silicon carbide based hard materials", pp. 683–748, Ch. 5 in *Handbook of Ceramic Hard Materials*. Ed. R. Riedel, Wiley-VCH Verlag GmbH, 2000.
22. W.J. Clegg, "Role of carbon in the sintering of boron-doped silicon carbide", *J. Am. Ceram. Soc.*, **83** (2000) 1039–1043.
23. M. Balog, K. Sedlackova, P. Zifcak, J. Janega, "Liquid phase sintering of SiC with rare-earth oxides", *Ceramics - Silikaty*, **49** (2005) 259–262.
24. S. Grasso, T. Saunders, H. Porwal, M. Reece, "Ultra-high temperature spark plasma sintering of α-SiC", *Ceram. Int.*, **41** (2015) 225–230.
25. A. Maître, A.V. Put, J.-P. Laval, S. Valette, G. Trolliard, "Role of boron on the Spark Plasma Sintering of an α-SiC powder", *J. Eur. Ceram. Soc.*, **28** (2008) 1881–1890.
26. F. Lomello, G. Bonnefont, Y. Leconte, N. Herlin-Boime, G. Fantozzi, "Processing of nano-SiC ceramics: Densification by SPS and mechanical characterization", *J. Eur. Ceram. Soc.*, **32** (2012) 633–641.
27. E. Ermer, P. Wiesław, S. Ludosław, "Influence of sintering activators on structure of silicon carbide", *Solid State Ionics*, **141** (2001) 523–528.
28. H. Tanaka, "Silicon carbide powder and sintered materials", *J. Ceram. Soc. Jpn.*, **119** (2011) 218–233.
29. S. Prochazka, R.M. Scanlan, "Effect of boron and carbon on sintering of SiC", *J. Am. Ceram. Soc.*, **58** (1975) 72.
30. R. Alliegro, L. Coffin, J. Tinklepaugh, "Pressure-sintered silicon carbide", *J. Am. Ceram. Soc.*, **39** (1956) 386–389.
31. K. Negita, "Effective sintering aids for silicon carbide ceramics: Reactivities of silicon carbide with various additives", *J. Am. Ceram. Soc.*, **69** (1986) C-308–C-310.
32. L. Stobierski, A. Gubernat, "Sintering of silicon carbide II. Effect of boron", *Ceram. Int.*, **29** (2003) 355–361.
33. V.-H. Nguyen, S.A. Delbari, M.S. Asl, Q. Van Le, A.S. Namini, Z. Ahmadi, M. Farvizi, M. Mohammadi, M. Shokouhimehr, "Combined role of SiC whiskers and graphene nano-platelets on the microstructure of spark plasma sintered ZrB_2 ceramics", *Ceram. Int.*, **47** (2021) 12459–12466.
34. R. Malik, Y.-W. Kim, "Pressureless solid-state sintering of SiC ceramics with BN and C additives", *J. Asian Ceram. Soc.*, **9** (2021) 1165–1172.
35. M. Liu, Y. Yang, Y. Wei, Y. Li, H. Zhang, X. Liu, Z. Huang, "Preparation of dense and high-purity SiC ceramics by pressureless solid-state-sintering", *Ceram. Int.*, **45** (2019) 19771–19776.
36. ASTM Standard, E494-10, "Standard practice for measuring ultrasonic velocity in materials", *ASTM International*, West Conshohocken, PA, 2010.
37. A. Montón, F. Maury, G. Chevallier, C. Estournès, M. Ferrato, D. Grossin, "Densification of surface-modified silicon carbide powder by spark-plasma-sintering", *J. Eur. Ceram. Soc.,* **41** (2021) 7543–7551.
38. C. Li, S. Li, D. An, Z. Xie, "Microstructure and mechanical properties of spark plasma sintered SiC ceramics aided by B_4C", *Ceram. Int.*, **46** (2020) 10142–10146.
39. J. Luo, R. Stevens, "Porosity-dependence of elastic moduli and hardness of 3Y-TZP ceramics", *Ceram. Int.*, **25** (1999) 281–286.